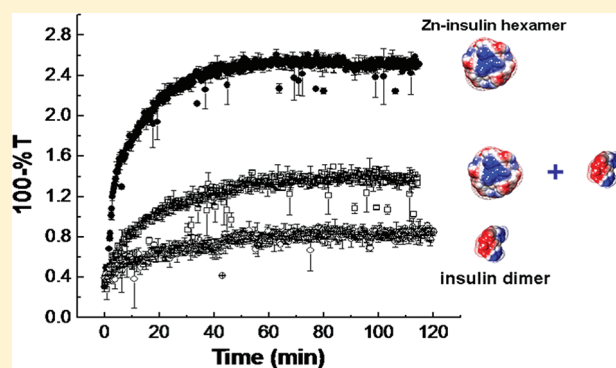


Multimerization and Aggregation of Native-State Insulin: Effect of Zinc

Yisheng Xu,[†] Yunfeng Yan,[†] Daniel Seeman,[†] Lianhong Sun,[‡] and Paul L. Dubin^{*,†}[†]Department of Chemistry, University of Massachusetts, 710 North Pleasant Street, Amherst, Massachusetts 01003, United States[‡]School of Life Sciences, University of Science and Technology of China, Hefei, Anhui 230027, People's Republic of China

Supporting Information

ABSTRACT: The aggregation of insulin is complicated by the coexistence of various multimers, especially in the presence of Zn^{2+} . Most investigations of insulin multimerization tend to overlook aggregation kinetics, while studies of insulin aggregation generally pay little attention to multimerization. A clear understanding of the starting multimer state of insulin is necessary for the elucidation of its aggregation mechanism. In this work, the native-state aggregation of insulin as either the Zn–insulin hexamer or the Zn-free dimer was studied by turbidimetry and dynamic light scattering, at low ionic strength and pH near pI. The two states were achieved by varying the Zn^{2+} content of insulin at low concentrations, in accordance with size-exclusion chromatography results and literature findings (Tantipolphan, R.; Romeijn, S.; Engelsman, J. d.; Torosantucci, R.; Rasmussen, T.; Jiskoot, W. J. *Pharm. Biomed.* 2010, 52, 195). The much greater aggregation rate and limiting turbidity (τ_{∞}) for the Zn–insulin hexamer relative to the Zn-free dimer was explained by their different aggregation mechanisms. Sequential first-order kinetic regimes and the concentration dependence of τ_{∞} for the Zn–insulin hexamer indicate a nucleation and growth mechanism, as proposed by Wang and Kurganov (Wang, K.; Kurganov, B. I. *Biophys. Chem.* 2003, 106, 97). The pure second-order process for the Zn-free dimer suggests isodesmic aggregation, consistent with the literature. The aggregation behavior at an intermediate Zn^{2+} concentration appears to be the sum of the two processes.



INTRODUCTION

The multimerization and aggregation of insulin are of great importance in biology,^{3,4} pharmacology,^{5,6} and protein fibrillogenesis.^{7–9} Insulin is stored in the pancreas as the inactive zinc hexamer.¹⁰ When released into the blood serum by the pH change, this hexamer dissociates into a dimer and then subsequently into a monomer,¹¹ which is its physiologically active form. However, the insulin monomer is less stable than the hexamer¹² and tends to aggregate.¹³ Although insulin is not one of the proteins whose amyloid is implicated in neurodegenerative diseases, it has nevertheless been used (with somewhat arbitrary incorporation of Zn) as a model for the etiology of fibril formation *in vitro* under conditions of extreme pH and temperature.^{14–17} It is likely that misfolded insulin monomers with exposed hydrophobic surfaces are involved in such amyloidogenesis.⁹ Because their precursors are native-state monomers, their role is expected to be diminished by the stabilization of the hexamer, most notably by the formation of the Zn complex. Thus, under physiological conditions, Zn–insulin shows reduced fibril formation relative to Zn-free insulin because of the formation of the stable Zn–insulin hexamer.^{18–20} It is important to have a firm understanding of the native-state multimerization equilibria of insulin in both the presence and absence of Zn^{2+} . An understanding of such equilibria under native conditions provides a foundation for the more elusive question of the behavior of

unfolded multimers. Experimentally, the equilibria among those multimers can be difficult to resolve from their tendency to aggregate. Therefore, there is a need to observe the causal relationship between native-state equilibria and aggregation, in the presence and absence of Zn^{2+} . In addition, such studies are relevant to the so-called low solubility (i.e., aggregation) of insulin and its impact on both the production of Zn–insulin and the subsequent bioactivity of its Zn-free form.

To understand why insulin aggregation under native-state conditions is sensitive to the presence or absence of Zn^{2+} , it is necessary to consider the multimerization of the insulin monomer and how Zn^{2+} affects those equilibria. Monomeric Zn-free insulin coexists with dimer, tetramer, hexamer, or other higher order multimers apparently in equilibrium.²¹ The notable absence of the trimer and pentamer indicate that the dimer is an elementary unit of higher order species. Such multimers are stable species and therefore, should be distinguished from the more generic “oligomers”, which may be formed by open-ended and possibly time-dependent linear association. The distribution of Zn–insulin or Zn-free multimers can be shifted toward lower order multimers (dimer or monomer) by decreasing pH,²² protein

Received: July 26, 2011

Revised: November 3, 2011

concentration,^{1,20,23} or ionic strength.²⁴ The effect of Zn^{2+} on multimer equilibria is dramatic because of the formation of a stable Zn–insulin complex, thought to arise from the combination of two Zn ions with three native conformation insulin dimers.^{12,25,26} Much like Zn-free insulin, the Zn-coordinated hexamer can also be in equilibrium with the monomer and dimer at neutral pH.^{21,27,28}

Effects of Zn^{2+} on native-state insulin aggregation were not at first coupled to its influence on multimer equilibria. Klostermeyer and Humbel found that excess Zn^{2+} results in the aggregation of insulin at pH > 4.²⁹ Grant et al. reported that the “solubility” (see above) of insulin decreased rapidly as the amount of Zn^{2+} added at neutral pH became sufficient to form hexamers complexed with 3–6 Zn^{2+} .³⁰ This “solubility” decrease after adding Zn^{2+} was explained by neutralization of net 12 negative charges on insulin hexamer at neutral pH by 6 Zn^{2+} .³¹ The zinc effect on aggregation was further supported by the fact that chelating Zn^{2+} by ethylenediaminetetraacetic tetrasodium salt (EDTA) slowed the aggregation of Zn–insulin (improved “solubility”).^{32,33} These observations subsequently led to proposals about the mechanism of aggregation, but controversy still exists concerning both the aggregating species (“reactant”) and the model best suited to describe its aggregation.

Several studies have addressed these two issues, i.e., aggregating species and model of aggregation. The situation is less controversial for Zn-free insulin, where the dimer is generally recognized as the predominant starting species,²⁵ either because it is the dominant multimer under typical conditions or it aggregates most rapidly (i.e., as a relatively unstable species whose aggregation depends upon pH and ionic strength³⁴). Further evidence that the dimer is the basic unit for further self-association comes from sedimentation studies of Zn-free insulin multimerization by Jeffrey et al.³⁵ The situation appears more complex for Zn–insulin. Grant et al. proposed that the Zn–insulin hexamer itself aggregates indefinitely, regardless of its equilibrium with the monomer and dimer.³⁰ On the other hand, Dathe et al. reported that the aggregation of Zn–insulin required dissociation of the Zn–insulin hexamer to the dimer.³⁶ Kinetic analysis of the aggregation of either the dimer or the Zn–insulin hexamer should describe the rate of depletion of such reactants, in accordance with several models of protein aggregation generally applied but not restricted to unfolded proteins. These include (1) simple growth, in which proteins oligomerize (including dimer, trimer, etc.) in a manner independent of the size of these oligomers,³⁷ (2) monomer–cluster aggregation, the addition of individual proteins to preformed protein aggregate,^{37–39} (3) cluster–cluster aggregation, in which aggregates of any size can combine, with no sequential addition of monomer units,³⁸ and (4) distinctive nucleation-controlled aggregation, in which sequential monomer addition takes place only after the cooperative formation of a cluster (nucleus).³⁷ If process (4) is slow, aggregation is “nucleation-dependent”,³⁹ as cited in ref 37. When positive cooperativity is introduced in process (2), exponential growth is observed.³⁷ An example of comprehensive integration of such sequential processes has been offered by Nicolai and co-workers⁴⁰ for the thermally induced aggregation of β -lactoglobulin (BLG). However, the variable use of terms, such as aggregate, cluster, oligomer, and multimer, can complicate comparisons of these models. In the present work, “multimers” are defined as thermodynamically stable inter-protein entities with uniquely defined structures. Interpretation of aggregation data may be incomplete without consideration of the multimer state, while descriptions of multimer equilibria can be erroneous if aggregation is not considered.

To further clarify the native-state aggregation mechanism of insulin, studies with known multimer conditions are required. Here, we focus on the aggregation of insulin at pH near pI (5.3), which is usually avoided because of the tendency of both Zn–insulin and Zn-free insulin to aggregate strongly under these conditions.^{41,42} We attempt to address two questions: (1) What are the most likely aggregating insulin species at different relative Zn^{2+} concentrations? (2) What are the aggregation pathways in the presence and absence of Zn^{2+} ? We investigate the effect on the multimer state of dilution at a fixed Zn/insulin ratio and the effect on aggregation of the zinc content, insulin concentration, and pH. Size-exclusion chromatography (SEC) and dynamic light scattering (DLS) are used to identify the multimer species before and during the aggregation. Aggregation rates are studied by turbidimetry and DLS. Analysis of time-dependent turbidity via the nucleation and growth model by Wang and Kurganov suggests different pathways for Zn–insulin and Zn-free insulin.

■ EXPERIMENTAL SECTION

Materials. Zn–insulin was a gift from the Eli Lilly Corporation. Zn-free insulin was prepared by dialyzing 15 mL of Zn–insulin (100 mg dissolved at pH 3.5) against pH 3.5 deionized (DI) water containing 0.1% EDTA at 4 °C for 48 h with two changes of the dialyzate.⁴³ Finally, dialysis against pH 3.5 DI water for 24 h removed EDTA. The Zn content of Zn-free insulin was found by inductively coupled plasma–optical emission spectroscopy (ICP–OES) (Optima 4300 PV) to be less than 0.02%. NaCl, sodium phosphate (monobasic), zinc acetate, EDTA, NaOH, and HCl solutions were purchased from Fisher Scientific. Milli-Q water was used in all sample preparations.

Turbidimetry. Insulin solutions of desired concentrations were prepared at pH 9.0 in 10 mM phosphate and filtered (0.22 μ m Millipore) at 25 °C. Turbidimetric titrations were carried out at 25 °C by the addition of either 1 N NaOH (forward titration) or 1 N HCl (backward titration) to a 10 mL solution with stirring and simultaneous monitoring of pH and transmittance. For the time-dependent experiments, insulin samples were dissolved at pH 7.0 and brought to the desired pH by the addition of 1 N HCl in 20 s. For samples with 60 μ M Zn, a stock solution of 12 mM Zn^{2+} was first added to reach the desired concentration. Transmittance of insulin solutions were measured using a Brinkmann PC 800 colorimeter equipped with a 2 cm path length fiber-optics probe and a 450 nm filter, and pH was measured with a Corning 240 pH meter. In the low turbidity range, 100-%T is approximately equal to turbidity and is presented simply as τ . After suitable warm-up, the instrument drift over this time period was verified as less than 0.05% T (i.e., <0.5 ppt).

SEC. SEC was carried out on a prepacked Superose 6 HR 10/30 column, using a HP1050 LC system equipped with a diode array detector (DAD), with 50 μ L injections at 25 °C. The mobile phase was 30 mM phosphate buffer (pH 5.9) at 0.40 mL/min. Insulin solutions at various concentrations were adjusted to pH 6 and injected directly after filtration. The column was calibrated with thyroglobulin (660 kDa), bovine serum albumin (66.5 kDa), ovalbumin (44 kDa), carbonic anhydrase (29 kDa), ribonuclease A (13.7 kDa), and acetone (58 Da), as shown in the Supporting Information.

DLS. DLS was carried out at 25 °C with a Malvern Zetasizer Nano ZS instrument equipped with a temperature control and using a 633 nm He–Ne laser for backscattering at 173°. The measurement duration was 15 s, and 11 measurements were averaged for each analysis. The distributions of the mean apparent translational diffusion coefficients (D_T) were determined by fitting the DLS autocorrelation functions using non-negative constrained least squares (NNLS). The distribution of apparent sizes d_h was obtained from the distribution of mean apparent

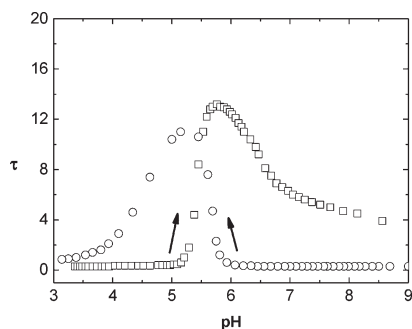


Figure 1. Turbidimetric titrations of $36 \mu\text{M}$ (0.2 g/L) Zn–insulin in $I = 10 \text{ mM}$ phosphate. Controlled rates of addition of acid or base titrant facilitated the interpretation of $(d\tau/dt)_{\text{pH}}$ in terms of the aggregation rate (see the text). Effect of the titration direction: (\square) low to high pH and (\circ) high to low pH.

translational diffusion coefficients (D_T) via

$$R_{\text{app}} = kT / (6\pi\eta D_T) \quad (1)$$

where k is the Boltzmann constant and η is the solvent viscosity, which was assumed to be that of water. In DLS, protein was dissolved in 10 mM phosphate buffer at $\text{pH } 8.0$ and $25 \text{ }^\circ\text{C}$ for at least 30 min . The protein solution was adjusted to the desired pH by NaOH and filtrated into a 1 mL low-volume cuvette using a Whatman $0.22 \mu\text{m}$ filter. Filtration, transfer, and automated optimization steps result in a delay of $3\text{--}4 \text{ min}$ between initial pH adjustment and the first measurement, as compared to delays of less than 20 s for turbidimetry.

Circular Dichroism (CD) Spectroscopy. CD spectra were obtained at $25 \text{ }^\circ\text{C}$ on a Jasco 720 CD spectropolarimeter with a Peltier temperature controller. A 0.4 g/L insulin solution was prepared in 10 mM phosphate at $\text{pH } 7.4$. Solutions of 0.4 g/L insulin corresponding to $\text{pH } 9.0$ and 3.0 were prepared by adjusting the pH using 1 N NaOH and HCl, respectively. Spectra were taken in the far-ultraviolet (UV) region ($200\text{--}250 \text{ nm}$) and in the near-UV region ($250\text{--}320 \text{ nm}$). Both far- and near-UV were recorded in a 0.1 cm quartz cell. Each spectrum was the result of three average scans.

RESULTS

Turbidimetric Acid–Base Titrations of Insulin. Figure 1 shows acid and base titrations for Zn–insulin in 10 mM phosphate, with the ionic strength that provides the maximum aggregation rate for Zn-free insulin.³⁴ Near- and far-UV CD spectra (see Figure S1 of the Supporting Information) confirm the preservation of the native state over this pH range, as expected from the results reported by Goldman and Carpenter.⁴⁴ Therefore, the differences in the two curves reflect the slow kinetics of dissolution at high pH of aggregates formed during titration with base. These aggregates are not identical to those formed during titration from high to low pH. Their dissolution at high pH is different from the eventual dissolution of aggregates formed by titration with acid. Initial pH values for both acid and base titrations correspond to native non-aggregated protein. Similar titrations previously performed with Zn-free insulin³⁴ show some resemblances but also important differences. Rate studies in ref 34 for Zn-free insulin show that the slopes of these curves at any pH $(d\tau/d\text{pH})_{\text{pH}}$ are proportional to the aggregation rate $(d\tau/dt)_{\text{pH}}$ because of the constancy of dV_{titrant}/dt and the near linearity of $d\text{pH}/dV_{\text{titrant}}$.³⁴ Consequently, the points of maximum turbidity correspond to the pH where rates of aggregation and disaggregation are equal. On the other hand, in

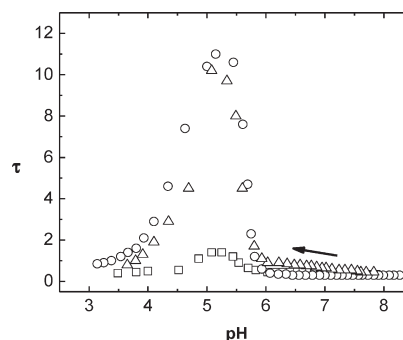


Figure 2. Effect of the Zn^{2+} content on titrations (from high to low pH) of (\circ) $36 \mu\text{M}$ (0.2 g/L) Zn–insulin (endogenous Zn) in buffer from Figure 1, (Δ) Zn-free insulin with additional (exogenous) $12 \mu\text{M}$ Zn^{2+} , and (\square) Zn-free insulin in 10 mM phosphate buffer. Note that first two have identical concentrations of Zn^{2+} (and insulin).

contrast to Zn-free insulin (see Figure S2 of the Supporting Information), both acid and base titration curves are asymmetric, the slope $(d\tau/dt)_{\text{pH}}$ is greater on the ascending side, indicating that the rate of aggregation or disaggregation as measured by turbidity is larger for the former. The points of maximum slope (ascending) are 5.4 (NaOH titration) and 5.6 (HCl titration). These observations indicate that the aggregating species are different at high and low pH.

The effect of Zn^{2+} is seen more clearly in Figure 2, which compares the acid titration of three solutions all with the same insulin concentration and ionic strength but differing with regard to the presence or absence of Zn^{2+} or with regard to sample history (endogenous or exogenous). We focus here on the forward (“high-to-low”) titrations to pass through physiological pH without aggregation. The titration curve for Zn-free insulin is essentially symmetrical and manifests much lower turbidity, a consequence of the low aggregation rate. In contrast, the results for (endogenous) Zn–insulin are asymmetric and display $10\times$ higher turbidity. While the titration of Zn-free insulin (at this pH and ionic strength dimer) is reversible, hence, the same regardless of the direction of the titration even at $180 \mu\text{M}$ (1 g/L),³⁴ the titration of Zn–insulin is not (Figure 1). In Figure 2, the solution of the Zn exogenous sample (Zn-free insulin to which Zn is added to achieve $[\text{Zn}^{2+}] = 12 \mu\text{M}$, identical to that in the Zn endogenous sample) gives a result identical to the Zn–insulin solution, demonstrating that Zn–insulin is in equilibrium with free Zn^{2+} , which thus may shift the multimer equilibria, a result consistent with the findings by Tantipolphan et al.¹ For this reason, we only need to consider the concentration of insulin and Zn/insulin total stoichiometry and not the Zn^{2+} content of the original protein.

SEC Analysis of the Insulin Association State. As seen from Figure 2, $36 \mu\text{M}$ (0.2 g/L) Zn–insulin, upon acidification, aggregates most rapidly at pH near pI, but this high velocity of aggregation requires sample dilution to obtain rates easily studied. However, lower concentrations for insulin and/or Zn^{2+} will shift the equilibrium to lower order multimer species.^{1,36,44,45} SEC as a function of the injection concentration for Zn–insulin in Figure 3A shows the coupled effect of these two variables (under eluent conditions that allow for both accurate column calibration and avoidance of aggregation, with the latter also assisted by on-column dilution). Given the continuous dilution during SEC, one can only estimate a reasonable range of effective dilutions during SEC, $10\text{--}20\times$.⁴⁵ From this estimate, we can

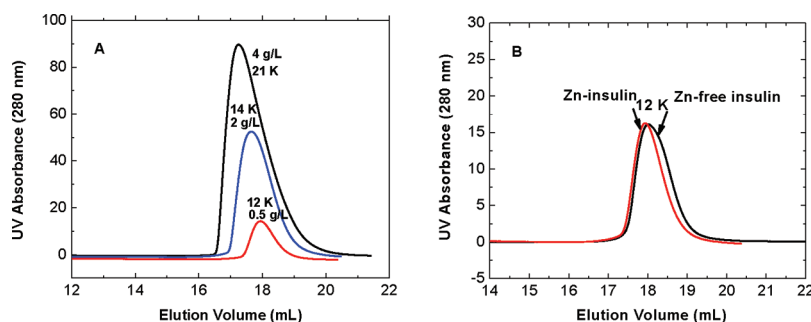


Figure 3. SEC elution profile of (A) Zn-insulin at different injection concentrations as shown and (B) Zn-insulin (from panel A) and Zn-free insulin, with a 0.5 g/L injection concentration, mobile phase pH 5.9, 30 mM phosphate buffer, and 50 μ L injection volume.

conclude from the result for the 90 μ M (0.5 g/L) injection that the dimer is the dominant species at $[\text{insulin}] < 9 \mu\text{M}$ (0.05 g/L) and $[\text{Zn}^{2+}] < 3 \mu\text{M}$ (0.018 g/L). On the other hand, the chromatogram at 4 g/L shows that obvious fronting is not representative of the initial distribution.⁴⁶ The “on-column concentration”⁴⁵ (4 g/L insulin injection) for insulin and Zn^{2+} are 36–72 μM (0.2–0.4 g/L) and 12–24 μM , respectively, probably leading to the formation of a mixture of hexamer and dimer prior to elution, leading to an apparent molecular weight (MW) of 21 kDa smaller than the expected hexamer MW of 34 kDa. These results are in accordance with previous studies that show that Zn-insulin concentrations higher than 36 μM (0.2 g/L) are required to preserve the hexamer.²⁸ The intermediate peak [injection concentration of 360 μM (2 g/L)] corresponds to a further shift in the equilibrium. Injection of either Zn-insulin or Zn-free insulin at 9 μM (0.5 g/L) followed by on-column dilution yields a dimer peak (Figure 3B). Even further dissociation of the dimer to the monomer has been observed for SEC injection of 0.06 g/L Zn-free insulin.¹⁸ These results demonstrate shifts in the multimer equilibria upon the dilution of endogenous Zn-insulin; the addition of excess Zn^{2+} is required to preserve the hexameric state (see Figure S3 of the Supporting Information).¹

Time Dependence of Insulin Aggregation. Figure 4 shows the aggregation of insulin at varying levels of $[\text{Zn}^{2+}]$ at a pH of 5.5, chosen to correspond to the maxima in $(d\tau/dt)$ from Figure 1. To compensate for this increased aggregation rate, we reduced the protein concentration from 36 μM (0.2 g/L) (Figure 1) to 9 μM (0.05 g/L) (note that this concentration is nearly 100 \times smaller than that required to make the hexamer, the predominant species in the absence of zinc⁴⁷). On the basis of the results by Tantipolphan et al.¹ from SEC with light scattering detection, we set the Zn^{2+} concentration to 60 μM in curve 3 to ensure that the Zn-insulin hexamer is the only species present under the conditions of curve 3; on the other hand, curve 1 corresponds to the Zn-free dimer, as shown in Figure 3B. Curve 2 corresponds to a stoichiometry of crystalline Zn-insulin itself. Curve 3 shows a particularly high aggregation rate in the first 5 min, followed by a plateau after 40 min. In contrast, a much lower aggregation rate and no obvious rapid initial phase are seen in curve 1. Curve 2 with $[\text{Zn}^{2+}]/[\text{insulin}] = 1:3$ represents an intermediate case and aggregates more strongly than Zn-free insulin.

The rapid increase in turbidity during the first 5 min for curve 3 in Figure 4 is reminiscent of the turbidimetric results for non-denatured BLG in low salt near the pH of maximum aggregation,⁴⁸ which was found to exhibit two apparent first-order regimes.

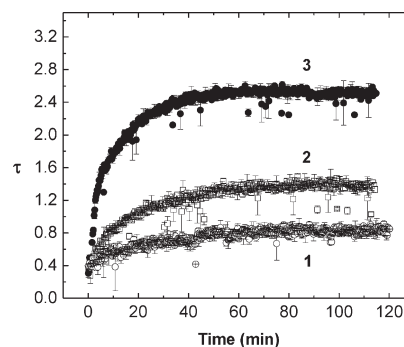


Figure 4. Time dependence of turbidity for 9 μM (0.05 g/L) insulin in $I = 10 \text{ mM}$ phosphate at pH 5.5. From top to bottom: (3) Zn-insulin with added 60 μM Zn^{2+} , (2) Zn-insulin, and (1) Zn-free insulin.

Such behavior has been explained by Wang and Kurganov and Kurganov et al. in terms of a nucleation and growth mechanism for firefly luciferase,^{2,49} and a detailed description of this process was included in a quantitative and thorough elucidation of the heat-induced aggregation of BLG by Nicolai et al.⁴⁰ We plot the results of Figure 4 in the manner of ref 48, limiting the data in Figure 5 to the first 40 min because a large error is introduced when the turbidity approaches its limiting value. According to Kurganov et al., the pseudo-first-order behavior^{49,50} of curve 3 in Figure 5A is a consequence of a nucleation step for the formation of protein clusters, followed by their incorporation of monomers without a change in the number of clusters. Such first-order plots follow eq 2

$$\tau = \tau_{\infty}(1 - e^{-kt}) \quad (2)$$

where τ is the turbidity (linear with 100-% T in the low turbidity range), which is assumed to be proportional to the amount of aggregate formed, τ_{∞} is the limiting value of τ at $t = \infty$, and k is the rate constant. This assumption is supported by a linear dependence of τ_{∞} upon the initial protein concentration seen in Figure 6B. While the proteins reported by Wang and Kurganov² may undergo unfolding, a similar two-step first-order plot was also observed for the native-state aggregation of BLG. Similar to the results reported by Wang and Kurganov,² there is a possible lag time of approximately 1 min for Zn-insulin, not seen in prior work with BLG.⁴⁸ The nucleation and growth model predicts a linear dependence of τ_{∞} upon the initial concentration^{2,49} and is seen in Figure 6 for insulin in the presence of excess Zn^{2+} . In contrast to the excess Zn^{2+} case (curve 3), Zn-free insulin (curve 1) clearly fits better to a second-order kinetic model. In Figure 5B,

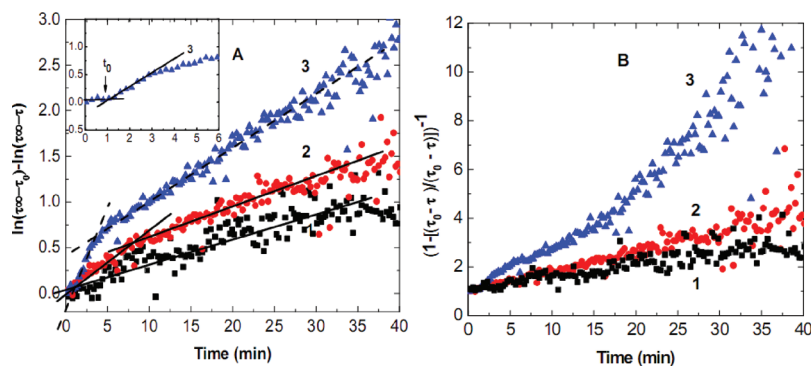


Figure 5. Kinetic fits of data from Figure 4: (A) first order and (B) second order, with (3) Zn–insulin adjusted to $60 \mu\text{M Zn}^{2+}$ (blue \blacktriangle), (2) Zn–insulin without added Zn (red \bullet), and (1) Zn-free insulin (black \blacksquare). The inset in panel A is an expanded time scale for Zn–insulin with $60 \mu\text{M Zn}^{2+}$ and indicates a lag time (t_0) of ca. 1 min.

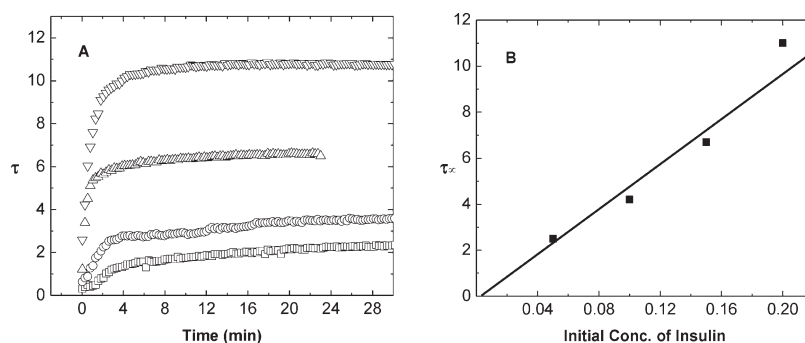


Figure 6. (A) Time dependence of turbidity for 9, 18, 27, and $36 \mu\text{M}$ (0.05, 0.1, 0.15, and 0.2 g/L) from bottom to top, with insulin at fixed $[\text{Zn}^{2+}]/[\text{insulin}] = 60:9$. (B) Turbidity maxima versus the initial insulin concentration derived from panel A.

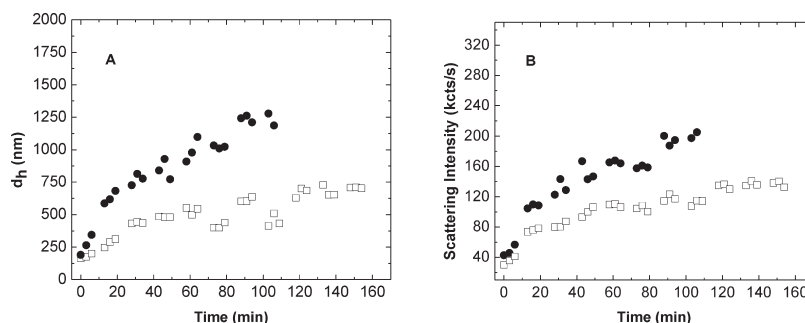


Figure 7. Time dependence of (A) hydrodynamic diameter and (B) scattering intensities of $9 \mu\text{M}$ (0.05 g/L) Zn–insulin in $I = 10 \text{ mM}$ phosphate, (\bullet) with and (\square) without $60 \mu\text{M}$ added Zn^{2+} . The initial pH was adjusted from pH 8.5 to 5.5.

a second-order analysis of the data of Figure 4 was also plotted, following eq 3.

$$\tau = \tau_{\infty} - \left(kt + \frac{1}{\tau_{\infty} - \tau_0} \right)^{-1} \quad (3)$$

To characterize the oligomeric precursors of aggregation, DLS was performed at conditions corresponding to Figure 4 (curves 3 and 2), i.e., $9 \mu\text{M}$ (0.05 g/L) insulin at pH 5.5 and Zn^{2+} concentrations of 60 and $3 \mu\text{M}$. The resulting panels A and B of Figure 7 for Zn–insulin ($60 \mu\text{M Zn}^{2+}$) show two regions, below and beyond 10 min. However, the scattering contribution from particles with sizes below 150 nm cannot be detected at this

insulin concentration. Note that the single mode reported for d_h represents an average of the fast and slow (“monomer” and aggregate) contributions, so that the increasing slope at $t > 20$ and the absence of a plateau compared to Figure 4A could come from monomer depletion (essentially an artifact of the use of the first cumulant). The high error also reflects this variability. To observe the fast mode more clearly, the concentration was increased by a factor of 40 ($360 \mu\text{M}$). Because such solutions almost immediately precipitate at pH 5.5, the pH was adjusted to 5.9, close to the onset of aggregation induced by acidification (Figure 1). The results are shown in panels A and B of Figure 8. Figures 7 and 8 differ in several ways, but for both, one sees an initial period, about 15–20 min for high Zn content curves, in

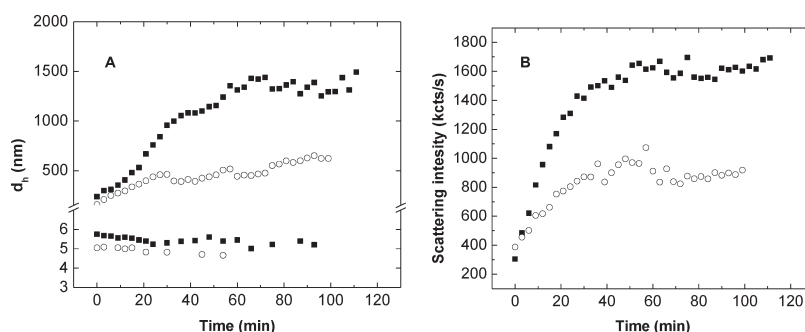


Figure 8. Time dependence of (A) d_h and (B) intensity of 360 μM (2 g/L) insulin, with (■) 120 μM Zn^{2+} and (○) 0 μM Zn^{2+} in pH 5.9. $I = 10$ mM phosphate buffer.

which size (d_h) increases from 150 to 500 nm. In the conditions of Figure 8, non-aggregated (fast-mode) species could be detected over the first hour for both Zn–insulin and Zn-free insulin (Figure 8A). A plateau is reached in Figure 8B for Zn–insulin after 30 min, similar to the result for Zn–insulin in Figure 4. Also after 30 min, the time dependence of the particle size is reduced, increasing from ca. 120 to 1100 nm in the first 30 min, only to ca. 1400 nm in the following 100 min, and essentially stable after 1 h. Both panels A and B of Figure 7 and Figure 8A show at ca. 10 min a break occurring in intensity or an increase in particle size >400 nm, but the higher concentration of Figure 8A appears to insert an additional feature between 15 and 30 min.

DISCUSSION

Zn-Induced Multimer Speciation and Aggregation. The much greater aggregation for Zn–insulin versus its Zn-free homologue is correlated with their different multimeric states. The major forms of insulin at different protein and Zn^{2+} concentrations are summarized in Figure S5 of the Supporting Information. The effect of Zn^{2+} on aggregation (often described in terms of “solubility”)^{30,31} has been noted, as well as the role of Zn^{2+} in multimer speciation, but there has previously been little mention of their correlation or causality. There are manifold effects on insulin multimer equilibria arising from the protein concentration,^{1,36,44,45} Zn/insulin stoichiometry,¹ pH,⁵¹ and ionic strength.²⁴ Nevertheless, the effects of Zn^{2+} on aggregation shown in Figure 4 can be attributed to the presence or absence of the Zn–insulin hexamer in a manner consistent with both our SEC results and the literature (most notably ref 1). While we cannot reject out of hand the possibility that curve 2 in Figure 1 corresponds to the Zn dimer, there is little evidence for the stability of this species.^{12,44}

Nucleation and Growth of the Zn–Insulin Hexamer. The difference in aggregation for the Zn–insulin hexamer and the Zn-free dimer from Figure 4 is best revealed from the kinetic plots of Figure 5: the aggregation starting from the Zn–insulin hexamer with excess Zn^{2+} (curve 3) displays two first-order regimes. This feature and the linear dependence of the limiting turbidity value τ_∞ on the initial concentration are consistent with the nucleation and growth mechanism described for the aggregation of firefly luciferase by Wang and Kurganov,² who account for the apparent first-order behavior of the two regimes. Here, in the first regime (<5 min), only nucleation occurs, with an observable increase in d_h from ca. 150 to 400 nm (Figure 7A). The decreased but non-zero time dependence of d_h at $t > 10$ min in Figure 7A suggests simultaneous nucleation and growth; in pure growth,

the aggregate size would be more limited because unaggregated proteins (“monomers”) only adsorb onto large particles (without a change in the number of nuclei) and these clusters do not aggregate with each other. The linearity of curve 3 in Figure 5 beyond 5 min results from the sum of the two apparent first-order kinetics. A near plateau in size characteristic of pure growth is seen after 40 min, at high insulin concentrations when the particle size exceeds $d_h = 1400$ nm (Figure 8A). This high-concentration condition also allows us to observe unaggregated hexameric units (but no higher oligomers), which appear to be fully depleted after 60 min. The multimerization equilibrium may be shifted to smaller species, with the concomitant decrease in both Zn concentrations and free insulin,^{1,36,44,45} as indicated by a small but significant decrease (6–5 nm in diameter) in d_h for the fast mode.

Nucleation of Zn–Insulin Hexamers: Aggregation versus Crystallization. The mechanism of Zn–insulin aggregation appears quite different from the aggregation of the Zn-free insulin pH dimer, as evident from the rate of aggregation, the kinetic order, and the symmetry and reversibility of the pH titration curves.³⁴ While Zn–insulin is evidently more susceptible to aggregation than the apo form, the mechanism of its aggregation and, in particular, the role of Zn^{2+} have not been fully resolved from “isoelectric precipitation”. As seen in Figure 1, the presence of Zn^{2+} does not change the principal signature of this form of aggregation, with the proximity to pI of the pH of maximum aggregation rate (inflection points of Figure 1).

The interactions among Zn–insulin hexamers responsible for aggregation are expected to be similar to those that promote crystallization.⁵² These interactions are likely to involve hexamer–hexamer interfacial aromatic interactions and hydrogen bonds, with a special role for residues near the hexamer cavity because those residues project beyond the hexamer surface plane.⁵³ We propose that similar quasi-ordered arrangements in solution lead to a cooperativity of binding, with a significant number of hexamers converging to form “clusters”, which are largely amorphous but with local interactions similar to those in crystals. In this micellization-like stage of nucleation-controlled aggregation,³⁷ smaller clusters are less stable than larger clusters; therefore, these clusters increase in size and number until the stage of pure nucleation is terminated, corresponding here to the break in curve 3 of Figure 5A at 4–5 min. Subsequently, growth continues mainly by the attachment of Zn–insulin hexamers (“particles”³⁷ or “monomers”²). Preservation of the linear relationship between total protein and limiting turbidity (Figure 6) suggests the absence of cluster–cluster aggregation,^{49,50} which may however occur at concentrations above 90 μM (0.5 g/L), where precipitation is observed.

Different Aggregation Mechanism for Zn-Free Insulin. Zn-free insulin shows pH-induced aggregation (as in Figure 2) independent of the direction of pH adjustment,³⁴ in contrast to Zn–insulin (Figure 1). The aggregation of the apo form appears to be second-order “simple” diffusion-limited controlled association (DLCA).³⁷ These differences can be related to the bilateral asymmetry of the insulin dimer, both electrostatically⁵⁴ and geometrically,⁵² which suggests isodesmic linear association.^{28,35} While the dimer is the initial species, there is no difference in bonding between the formation of the insulin dimer and its hypothetical growth to the tetramer or the addition of protein to any other linear oligomer. For such oligomerization $d + d_n \rightarrow d_{n+1}$ or $d_n + d_q \rightarrow d_{n+q}$ (where d is the dimer), kinetics should be second-order, as supported by Figure 5B. Intermediate oligomers can be detected by ultracentrifugation,⁵¹ although not by scattering under conditions at which aggregates dominate the signal (high protein concentration, $t > 4$ min). In contrast, Zn binding confers unique stability to a hexamer, which then nucleates rapidly; therefore, clusters of size between hexamer and 150–600 nm nuclei are unstable and, thus, undetected. Nuclear magnetic resonance (NMR) studies indicate that Zn–insulin at this same concentration contains observable amounts of hexamer, absent in the dimeric Zn-free insulin,²¹ (curve 1 in Figure 4). Hence, these data represent a combination of hexameric and dimeric insulin. At lower concentrations, the former accounts for the lower slope and longer duration of the nucleation period in curve 2 compared to curve 3.

CONCLUSION

The speciation of insulin is controlled by the protein concentration and strongly influenced by Zn^{2+} , and this controls aggregation. The predominant species in the presence and absence of 60 μM Zn^{2+} are the Zn–insulin hexamer and the Zn-free dimer, respectively. The higher turbidities and rates of aggregation for the former correspond to nucleation and growth, as opposed to second-order diffusion-limited aggregation for the latter. The balance among the various equilibrium multimers is modulated by both insulin and Zn^{2+} concentrations.

The optimal values needed to define multimer species were identified by SEC. Both the Zn–insulin hexamer and the Zn-free dimer show “isoelectric precipitation”, indicating suppression of aggregation by charge repulsion. However, it is suggested that the interaction between the associating dimers in the absence of Zn^{2+} follows an isodesmic pathway that accommodates progressive oligomerization, whereas the unique structure, stability, and tendency toward crystallization of the Zn–insulin hexamer promotes strong initial formation of clusters that serve as nuclei for subsequent growth. Aggregation at a low Zn^{2+} concentration reflects both of these mechanisms. These findings may support further consideration of equilibrium multimers as the starting points of irreversible aggregation (amyloid and fibril formation) and emphasize the need to distinguish time-independent oligomerization from equilibrium speciation. Studies in progress at elevated temperatures in the presence of heparin should indicate how this aggregation suppressor³⁴ may enter into the pathways proposed here.

ASSOCIATED CONTENT

S Supporting Information. CD spectra on insulin at various pH conditions, forward and reverse pH titration curves of

Zn-free insulin, apparent MWs of insulin as a function of the protein concentration eluted from SEC with and without excess zinc in mobile phase, SEC elution profile and calibration curve of protein standards, and the major forms of insulin at different protein and Zn^{2+} concentrations. This material is available free of charge via the Internet at <http://pubs.acs.org>.

AUTHOR INFORMATION

Corresponding Author

*E-mail: dubin@chem.umass.edu.

ACKNOWLEDGMENT

Support from the National Science Foundation (NSF) (Grant CBET-0966923) is acknowledged. We thank the Eli Lilly Corporation for the gift of Zn–insulin. We also thank Prof. Wim Jiskoot for allowing us to include data from his publication in our Supporting Information.

REFERENCES

- (1) Tantipolphan, R.; Romeijn, S.; Engelsman, J. d.; Torosantucci, R.; Rasmussen, T.; Jiskoot, W. *J. Pharm. Biomed.* **2010**, *52*, 195.
- (2) Wang, K.; Kurganov, B. I. *Biophys. Chem.* **2003**, *106*, 97.
- (3) Kahn, C. R.; Baird, K. L.; Jarrett, D. B.; Flier, J. S. *Proc. Natl. Acad. Sci. U.S.A.* **1978**, *75*, 4209.
- (4) Pezron, I.; Mitra, R.; Pal, D.; Mitra, A. K. *J. Pharm. Sci.* **2002**, *91*, 1135.
- (5) Costantino, H. R.; Langer, R.; Klivanov, A. M. *Pharm. Res.* **1994**, *11*, 21.
- (6) Cromwell, M. E.; Hilario, E.; Jacobson, F. *AAPS J.* **2006**, *8*, E572.
- (7) Hua, Q.-x.; Weiss, M. A. *J. Biol. Chem.* **2004**, *279*, 21449.
- (8) Groenning, M.; Frokjaer, S.; Vestergaard, B. *Curr. Protein Pept. Sci.* **2009**, *10*, 509.
- (9) Lee, C.-C.; Nayak, A.; Sethuraman, A.; Belfort, G.; McRae, G. J. *Biophys. J.* **2007**, *92*, 3448.
- (10) Bryant, C.; Spencer, D. B.; Miller, A.; Bakaysa, D. L.; McCune, K. S.; Maple, S. R.; Pekar, A. H.; Brems, D. N. *Biochemistry* **1993**, *32*, 8075.
- (11) Dodson, G.; Steiner, D. *Curr. Opin. Struct. Biol.* **1998**, *8*, 189.
- (12) Dunn, M. F. *Biometals* **2005**, *18*, 295.
- (13) Chiti, F.; Dobson, C. M. *Annu. Rev. Biochem.* **2006**, *75*, 333.
- (14) Nielsen, L.; Khurana, R.; Coats, A.; Frokjaer, S.; Brange, J.; Vyas, S.; Uversky, V. N.; Fink, A. L. *Biochemistry* **2001**, *40*, 6036.
- (15) Dyukov, M.; Grudin, M.; Sirotkin, A.; Kiselev, O. *Dokl. Biochem. Biophys.* **2008**, *419*, 79.
- (16) Ahmad, A.; Uversky, V. N.; Hong, D.; Fink, A. L. *J. Biol. Chem.* **2005**, *280*, 42669.
- (17) Jansen, R.; Dzwolak, W.; Winter, R. *Biophys. J.* **2005**, *88*, 1344.
- (18) Andra, N.; Julia, G.; Julia, S.; Vello, T.; Peep, P. *Biochem. J.* **2010**, *430*, 511.
- (19) Nielsen, L.; Frokjaer, S.; Brange, J.; Uversky, V. N.; Fink, A. L. *Biochemistry* **2001**, *40*, 8397.
- (20) Somasundaran, P. *Encyclopedia of Surface and Colloid Science*; CRC Press (Taylor and Francis Group): Boca Raton, FL, 2006; Vol. 5, p 5274.
- (21) Bocian, W.; Sitkowski, J.; Tarnowska, A.; Bednarek, E.; Kawęcki, R.; Koźmiński, W.; Kozerski, L. *Proteins: Struct., Funct., Bioinf.* **2008**, *71*, 1057.
- (22) Lord, R. S.; Gubensek, F.; Rupley, J. A. *Biochemistry* **1973**, *12*, 4385.
- (23) Pekar, A. H.; Frank, B. H. *Biochemistry* **1972**, *11*, 4013.
- (24) Kadima, W.; Øgendal, L.; Bauer, R.; Kaarsholm, N.; Brodersen, K.; Hansen, J. F.; Porting, P. *Biopolymers* **1993**, *33*, 1643.
- (25) Pocker, Y.; Biswas, S. B. *Biochemistry* **1981**, *20*, 4354.

- (26) Brange, J.; Andersen, L.; Laursen, E. D.; Meyn, G.; Rasmussen, E. *J. Pharm. Sci.* **1997**, *86*, 517.
- (27) Jeffrey, P. D. *Biochemistry* **1974**, *13*, 4441.
- (28) Attri, A. K.; Fernández, C.; Minton, A. P. *Biophys. Chem.* **2010**, *148*, 23.
- (29) Klostermeyer, H.; Humbel, R. E. *Angew. Chem., Int. Ed.* **1966**, *5*, 807.
- (30) Grant, P. T.; Coombs, T. L.; Frank, B. H. *Biochem. J.* **1972**, *126*, 433.
- (31) Emdin, S.; Dodson, G.; Cutfield, J.; Cutfield, S. *Diabetologia* **1980**, *19*, 174.
- (32) Blundell, T.; Dodson, G.; Hodgkin, D.; Mercola, D. *Adv. Protein Chem.* **1972**, *26*, 279.
- (33) Quinn, R.; Andrade, J. D. *J. Pharm. Sci.* **1983**, *72*, 1472.
- (34) Giger, K.; Vanam, R. P.; Seyrek, E.; Dubin, P. L. *Biomacromolecules* **2008**, *9*, 2338.
- (35) Jeffrey, P. D.; Milthorpe, B. K.; Nichol, L. W. *Biochemistry* **1976**, *15*, 4660.
- (36) Dathe, M.; Gast, K.; Zirwer, D.; Welfle, H.; Mehlis, B. *Int. J. Pept. Protein Res.* **1990**, *36*, 344.
- (37) De Young, L. R.; Fink, A. L.; Dill, K. A. *Acc. Chem. Res.* **1993**, *26*, 614.
- (38) Khanova, H. A.; Markossian, K. A.; Kurganov, B. I.; Samoilov, A. M.; Kleimenov, S. Y.; Levitsky, D. I.; Yudin, I. K.; Timofeeva, A. C.; Muranov, K. O.; Ostrovsky, M. A. *Biochemistry* **2005**, *44*, 15480.
- (39) Speed, M. A.; King, J.; Wang, D. I. C. *Biotechnol. Bioeng.* **1997**, *54*, 333.
- (40) Le Bon, C.; Nicolai, T.; Durand, D. *Macromolecules* **1999**, *32*, 6120.
- (41) Tanford, C.; Epstein, J. *J. Am. Chem. Soc.* **1954**, *76*, 2170.
- (42) Tanford, C.; Epstein, J. *J. Am. Chem. Soc.* **1954**, *76*, 2163.
- (43) Kwon, Y. M.; Baudys, M.; Knutson, K.; Kim, S. W. *Pharm. Res.* **2001**, *18*, 1754.
- (44) Goldman, J.; Carpenter, F. H. *Biochemistry* **1974**, *13*, 4566.
- (45) Jorgensen, L.; Bennedsen, P.; Hoffmann, S. V.; Krogh, R. L.; Pinholt, C.; Groenning, M.; Hostrup, S.; Bukrinsky, J. T. *Eur. J. Pharm. Sci.* **2011**, *42*, 509.
- (46) Yu, C.-M.; Mun, S.; Wang, N.-H. L. *J. Chromatogr., A* **2008**, *1192*, 121.
- (47) Hansen, J. F. *Biophys. Chem.* **1991**, *39*, 107.
- (48) Majhi, P. R.; Ganta, R. R.; Vanam, R. P.; Seyrek, E.; Giger, K.; Dubin, P. L. *Langmuir* **2006**, *22*, 9150.
- (49) Kurganov, B. I.; Rafikova, E. R.; Dobrov, E. N. *Biochemistry (Moscow)* **2002**, *67*, 525.
- (50) Kurganov, B. I. *Biochemistry (Moscow)* **2002**, *67*, 409.
- (51) Mark, A. E.; Nichol, L. W.; Jeffrey, P. D. *Biophys. Chem.* **1987**, *27*, 103.
- (52) Turkenburg-van Diepen, M. Ph.D. Thesis, Department of Chemistry, University of York, York, U.K., 1996.
- (53) Yip, C. M.; Brader, M. L.; DeFelippis, M. R.; Ward, M. D. *Biophys. J.* **1998**, *74*, 2199.
- (54) Seyrek, E.; Dubin, P. L.; Tribet, C.; Gamble, E. A. *Biomacromolecules* **2003**, *4*, 273.